

# Synthesis of ZnSnO<sub>3</sub> nanocubes and thin film fabrication of (ZnSnO<sub>3</sub>/PMMA) composite through electrospray deposition

Kyung Hyun Choi<sup>1</sup> · Ghayas Uddin Siddiqui<sup>1</sup> · Bong-su Yang<sup>1</sup> · Maria Mustafa<sup>2</sup>

Received: 26 December 2014 / Accepted: 30 March 2015 / Published online: 20 May 2015  
© Springer Science+Business Media New York 2015

**Abstract** A composite of zinc stannate (ZnSnO<sub>3</sub>) nanocubes and poly(methyl methacrylate) (PMMA) has been prepared and deposited on a flexible substrate polyethylene terephthalate (PET) through electrospray deposition (ESD). This fabrication technique has been found very effective for deposition of this composite as thin film. ZnSnO<sub>3</sub> is an inorganic biocompatible and piezoelectric material while PMMA is a transparent and durable organic polymer material. ZnSnO<sub>3</sub> nanocubes have been synthesized via an aqueous solution method and ZnSnO<sub>3</sub>/PMMA composite has been deposited as thin film on PET through ESD. The average layer thickness of the as deposited ZnSnO<sub>3</sub>/PMMA composite film on PET was found to be 149 nm. Morphological and structural characterization of ZnSnO<sub>3</sub> nanocubes through FESEM and XRD showed its size uniformity and crystalline nature. The size of the ZnSnO<sub>3</sub> nanocubes was estimated by FESEM analysis which was around 50–70 nm. The chemical composition has been investigated with the help of FTIR and Raman spectroscopy. The optical characterization of as deposited ZnSnO<sub>3</sub>/PMMA composite film through UV/Vis spectroscopy showed an average transmittance of around 92 % and electrical characterization exhibited resistivity of approximately  $50 \times 10^5 \Omega \text{ cm}$ . This dielectric nature of

ZnSnO<sub>3</sub>/PMMA composite film indicates that this composite material can be employed as dielectric layer in printed electronics.

## 1 Introduction

In the field of research and development more attention is being paid towards the bio-compatible materials and their applications in daily life. In this regard, the lead free materials are getting more consideration and zinc stannate is one of them. Zinc stannate is a lead free piezoelectric and ferroelectric material which belongs to non-centrosymmetric (NCS) oxides, having perovskite structure. Zinc stannate nanostructures have the potential to be used in numerous device applications such as nanogenerators [1–3], sensors [4–7], transistors [8, 9], solar cells [10, 11] etc. Zinc stannate exists in two crystalline forms, trigonal ilmenite (ZnSnO<sub>3</sub>) [12] and cubic spinel (Zn<sub>2</sub>SnO<sub>4</sub>) [13]. In this research work, ZnSnO<sub>3</sub> has been studied involving its synthesis and its composite with PMMA. ZnSnO<sub>3</sub> nanostructures can be synthesized by different methods, including low temperature ion exchange [12], co-precipitation [14], thermal evaporation [15] and low-temperature solution-phase [16], and hydro-thermal methods [4]. We have synthesized ZnSnO<sub>3</sub> nanocubes via an aqueous solution method followed by vacuum filtration and calcination.

Atactic poly(methyl methacrylate) (PMMA) has a distinct place among other polymers because it has high resistance to UV light, greatest surface hardness of all thermoplastics and can be fabricated by all thermoforming methods. Chemically, it is the synthetic polymer of methyl methacrylate and often generically called acrylic glass. PMMA is one of the prominent polymers used in electronic devices such as dielectric in organic thin film transistors

✉ Kyung Hyun Choi  
amm@jejunu.ac.kr

<sup>1</sup> Department of Mechatronics Engineering, Jeju National University, Jeju, South Korea

<sup>2</sup> Department of Chemical Engineering, COMSATS Institute of Information Technology, Lahore, Pakistan

(OTFTs) [17], advanced electronics and optoelectronics [18], and as an optical lens in cameras and optical fibers [19].

Inorganic–organic composite materials are promising systems for a variety of applications due to their extraordinary properties, which arise from the synergism between the properties of the components. There are several routes to these materials, but probably the most prominent one is the incorporation of inorganic nanostructures in organic polymers. These materials have gained much interest due to the remarkable change in properties such as mechanical [20], thermal [21], electrical [22], and magnetic [23] compared to pure organic polymers. The novelty of our research work is that we have made a composite of ZnSnO<sub>3</sub>/PMMA and fabricated its thin film through a non-vacuum based inkjet printing technology i.e. ESD which is reliable, cost-effective and robust technique for fabrication of thin films at atmospheric conditions [24–32]. We first synthesized ZnSnO<sub>3</sub> nanocubes with an average size of 50–70 nm via an aqueous solution method which is cost effective and feasible method, first it involves the synthesis of zinc hydroxystannate (ZnSn(OH)<sub>6</sub>) as an intermediate product which after calcination converts to ZnSnO<sub>3</sub>. We investigated the compositional, morphological and structural properties of as synthesized ZnSn(OH)<sub>6</sub> and ZnSnO<sub>3</sub> nanocubes by field emission scanning electron microscopy (FE-SEM), X-ray diffraction (XRD), fourier transform infrared spectroscopy (FTIR) and Raman spectroscopy respectively. The structural, morphological, optical and electrical properties of ZnSnO<sub>3</sub>/PMMA thin film were investigated by FTIR, FE-SEM, UV/Vis/NIR spectrophotometer and semiconductor device analyzer respectively.

## 2 Experimental section

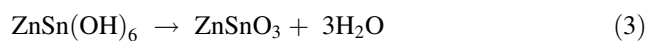
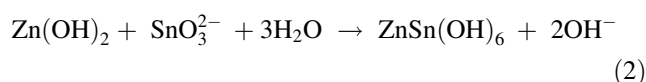
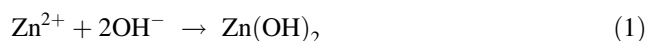
### 2.1 Materials and methods

For the synthesis of ZnSnO<sub>3</sub> nanocubes, the precursor zinc sulfate heptahydrate (ZnSO<sub>4</sub>·7H<sub>2</sub>O) (F. wt 287.56) and sodium stannate trihydrate (Na<sub>2</sub>SnO<sub>3</sub>·3H<sub>2</sub>O) (F. wt 266.71) were purchased from Duksan Pure Chemicals, South Korea and Junsei Chemical Co., Ltd. Japan respectively. For the synthesis of poly(methyl methacrylate) (PMMA) (mol wt of repeat unit 100.12) solution, PMMA powder and solvent (toluene or C<sub>7</sub>H<sub>8</sub>) were purchased from Sigma Aldrich, South Korea.

### 2.2 Preparation of ZnSnO<sub>3</sub>/PMMA ink

First the PMMA solution was prepared by dissolving 0.10 g of PMMA in 10 ml of toluene and kept on bath sonicator for 5 min and then kept for stirring at 40 °C for

24 h. And for the synthesis of crystalline ZnSnO<sub>3</sub> nanocubes via aqueous solution method, 100 mol of ZnSO<sub>4</sub>·7H<sub>2</sub>O were added in 100 ml of deionized (DI) water and stirred at room temperature until the complete dissolution of ZnSO<sub>4</sub>·7H<sub>2</sub>O. Then 100 mmol of Na<sub>2</sub>SnO<sub>3</sub>·3H<sub>2</sub>O were added into the preliminary solution and was kept on magnetic stirrer at 80 °C for 5 h. A white suspension of an intermediate product ZnSn(OH)<sub>6</sub> was formed which precipitates were collected from the solution by vacuum filtration and were washed with DI water several times to remove residual products and were then dried in air at 100 °C for 1 h. Afterwards, the as synthesized ZnSn(OH)<sub>6</sub> powder was calcinated at 600 °C for 3 h. Finally, we got the ZnSnO<sub>3</sub> nanocubes by the following possible reaction:



The as synthesized ZnSO<sub>3</sub> nanocubes were then dispersed in PMMA solution. For the better dispersion of ZnSnO<sub>3</sub> nanocubes into PMMA solution, it was sonicated for 30 min and a non-ionic surfactant, i.e. 0.01 % Triton X-100 (Sigma Aldrich) was also added for the same purpose and kept on stirrer at room temperature for overnight to check the stability of the synthesized ink. To improve the quality of the film and to meet the conductivity requirements for electrospray deposition, the co-solvent approach was adopted [28, 33] and dimethyl sulfoxide (DMSO) was added to ZnSnO<sub>3</sub>/PMMA ink in a ratio of 1:5.

### 2.3 Fabrication of ZnSnO<sub>3</sub>/PMMA composite film

ZnSnO<sub>3</sub>/PMMA thin film was deposited on a transparent substrate PET by using ESD. The PET substrates were cleaned by chemical etching followed by UV cleaning and oxygen plasma treatment before deposition of the film. First, the PET was immersed in a solution of sodium hydroxide (NaOH) (20 pbw) and distilled water (80 pbw) for 10 min at 80 °C followed by rinsing with hot water and drying in hot air. Then it was further rinsed with acetone and distilled water for 10 min each followed by UV/Ozone cleaning for 10 min and oxygen plasma cleaning for 1 min. The ZnSnO<sub>3</sub>/PMMA ink was filled in a glass syringe which was then fixed into a syringe pump by which flow rate of the ink was controlled. The syringe was connected to the metallic nozzle of diameter 110 μm through the Teflon tube. A high voltage source was applied between the metallic nozzle (anode) and the moving ground (cathode) upon which the substrate was placed. A high speed camera

was set to view the phenomena of electrospray. After setting all the instruments, the flow rate of 200  $\mu\text{l/h}$  was given to the ink and voltage was applied between the nozzle and moving ground. As the ink came into the nozzle, voltage was increased and the stable cone jet was achieved between 3.9 and 4.6 kV. The distance between the nozzle and the substrate (stand-off distance) was set at 20 mm. The as deposited  $\text{ZnSnO}_3/\text{PMMA}$  composite film on PET was sintered at 120  $^\circ\text{C}$  in a furnace for 3 h. The thickness of the  $\text{ZnSnO}_3/\text{PMMA}$  composite film was measured at different points and thus the average thickness of the film was found to be approximately 149 nm.

#### 2.4 Characterization techniques

The surface morphology and microstructure of  $\text{ZnSnO}_3$  nanocubes and  $\text{ZnSnO}_3/\text{PMMA}$  thin film were investigated by field emission scanning electron microscopy (FE-SEM) (JEOL JSM-7600F, Japan). The phase and crystalline orientation of  $\text{ZnSn}(\text{OH})_6$  and  $\text{ZnSnO}_3$  nanocubes were determined by the X-ray diffraction (XRD), Rigaku D/MAX 2200H diffractometer with  $\text{Cu K}\alpha$  radiation ( $\lambda = 1.5406 \text{ \AA}$ , 40 kV, 250 mA,  $8^\circ \text{ min}^{-1}$ ) using a fixed glancing incidence angle ( $2^\circ$ ). The FTIR spectra were recorded on Nicolet 6700 FT-IR spectrophotometer by using the pellets of sample mixed with KBr (0.5:100). Raman spectra were recorded on LabRAM HR Raman spectrometer with a solid state laser at room temperature. The thickness of the film was measured by a non-destructive thin film thickness measurement system Gaertner L116D ellipsometer. The optical properties of the  $\text{ZnSnO}_3/\text{PMMA}$  thin film were measured by using an ultraviolet–visible–near infrared (UV–Vis–NIR) spectrophotometer (Shimadzu UV 3150PC) at various wavelengths. Finally, the electrical properties of the  $\text{ZnSnO}_3/\text{PMMA}$  thin film

were measured by taking the current–voltage ( $I$ – $V$ ) graph through semiconductor device analyzer (agilent B1500A).

### 3 Results and discussion

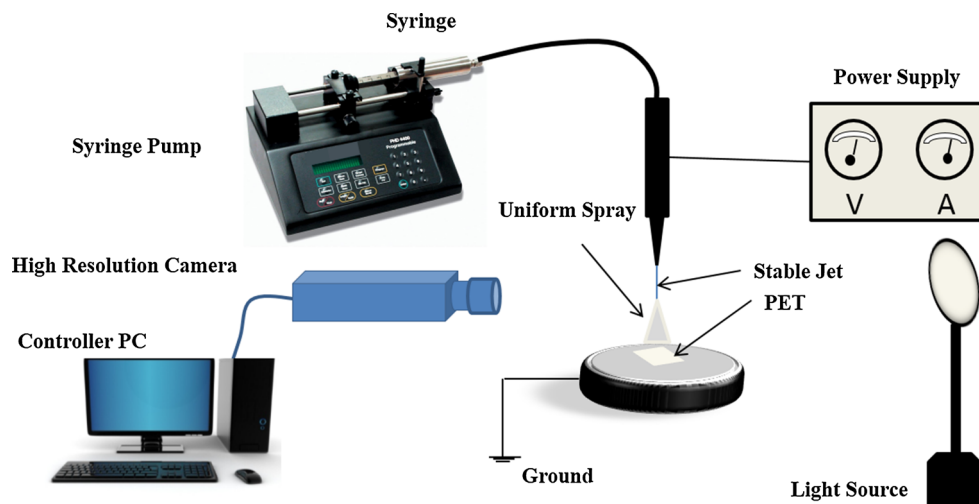
#### 3.1 Spray formation by ESD

The  $\text{ZnSnO}_3/\text{PMMA}$  ink was sprayed on PET by ESD as shown in the schematic diagram in Fig. 1. A uniform spray is necessary for the uniform film on the substrate that can be achieved only by a stable cone jet or Taylor Cone [34]. Three different modes of ESD, i.e. unstable, stable and multi jets were obtained and an operating envelope was explored between different flow rates and voltages which is shown in Fig. 2. In order to determine the spray conditions on a fixed stand-off distance of 20 mm, the spray was observed by varying the flow rates from 50 to 300  $\mu\text{l/h}$  and we performed this experiment with a flow rate of 200  $\mu\text{l/h}$ .

#### 3.2 Morphological and structural characterization

As described earlier in the experimental section, the morphology of the as synthesized  $\text{ZnSnO}_3$  nanocubes was investigated by FE-SEM as shown in Fig. 3. It reveals clearly the cubic shape of  $\text{ZnSnO}_3$  nanostructures having an average size of approximately 50–70 nm and also showing the large-scale, uniform cubic crystallites yielded with this approach. An intermediate product zinc hydroxystannate ( $\text{ZnSn}(\text{OH})_6$ ) is formed before the yield of  $\text{ZnSnO}_3$  nanocubes. They were obtained by carrying out the chemical reaction between  $\text{ZnSO}_4 \cdot 7\text{H}_2\text{O}$  and  $\text{Na}_2\text{SnO}_3 \cdot 3\text{H}_2\text{O}$  at 80  $^\circ\text{C}$  for 5 h which on further calcination at 600  $^\circ\text{C}$  for 3 h converted to the desired product, i.e.  $\text{ZnSnO}_3$  nanocubes. Figure 4a shows the XRD patterns of the

**Fig. 1** Schematic diagram of the electrospray deposition (ESD) system used for the deposition of  $\text{ZnSnO}_3/\text{PMMA}$  composite film on PET



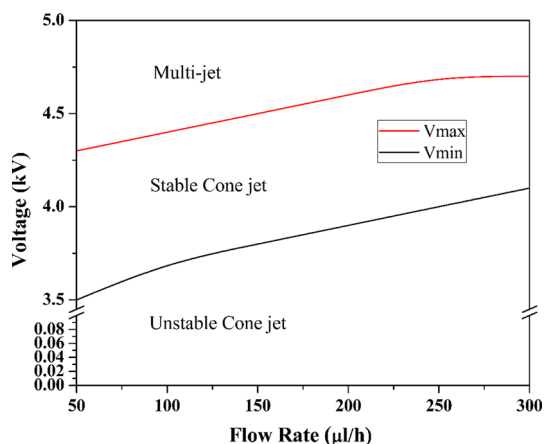


**Fig. 2** Operating envelope illustration of stable cone-jet mode between minimum and maximum applied potential depending upon the flow rate

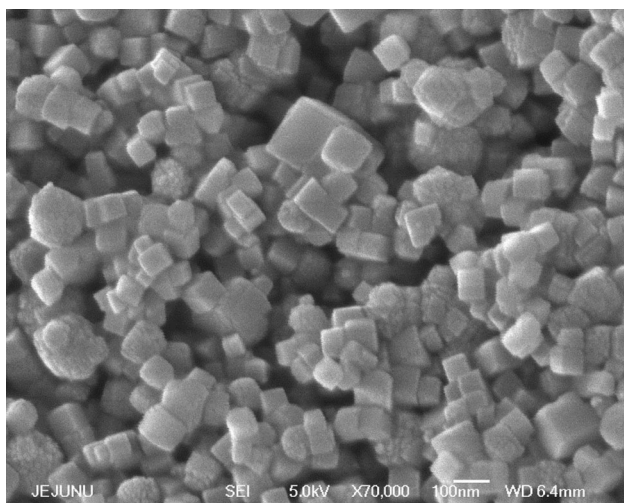


**Fig. 3** FE-SEM image of as grown  $\text{ZnSnO}_3$  nanocubes via an aqueous solution method

$\text{ZnSn(OH)}_6$  material obtained at  $80^\circ\text{C}$ . All the diffraction peaks are in good agreement with the values reported previously [35]. The crystalline structure of  $\text{ZnSnO}_3$  nanocubes is confirmed by XRD as shown in Fig. 4b, all of the indicating diffraction peaks can be indexed to the JCPDS card no. 28-1486. The XRD spectrum also indicates that  $\text{ZnSnO}_3$  nanocubes have pure crystalline structure and there are no impure phases in it. So overall it shows a large surface area, high crystallinity, smaller particle size and uniform morphology. FE-SEM image of  $\text{ZnSnO}_3$ /PMMA composite film in Fig. 5. indicates that the film surface is mainly covered by the PMMA and  $\text{ZnSnO}_3$  nanocubes are buried under thin layer.

To investigate the composition of  $\text{ZnSn(OH)}_6$  and  $\text{ZnSnO}_3$  Raman and FTIR spectra were obtained and obtained values of both spectra resemble well with the values

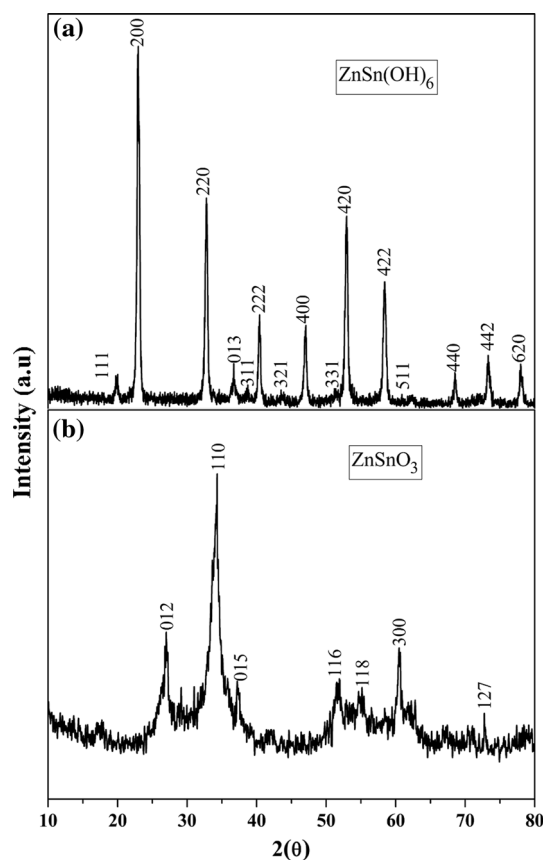


**Fig. 4** a XRD patterns of  $\text{ZnSn(OH)}_6$  synthesized via an aqueous solution method at  $80^\circ\text{C}$ . b XRD patterns of  $\text{ZnSnO}_3$  nanocubes obtained after the calcination at  $600^\circ\text{C}$

reported in literature [5, 36]. Figure 6 represents the Raman spectra of both materials  $\text{ZnSn(OH)}_6$  and  $\text{ZnSnO}_3$  in which four Raman modes can be seen at  $299$ ,  $372$ ,  $436$  and  $608\text{ cm}^{-1}$  for  $\text{ZnSn(OH)}_6$  arising from the breathing vibrations of the long M–OH bonds and M–OH–M (bridging OH group) bending modes. After heating the  $\text{ZnSn(OH)}_6$  at  $600^\circ\text{C}$  for 3 h the above mentioned four Raman modes were slightly shifted to two new Raman modes at  $538$  and  $671\text{ cm}^{-1}$ . The broad peak at  $671\text{ cm}^{-1}$  corresponds to the distinctive Raman shift of  $\text{ZnSnO}_3$  and is imputed to stretching vibrations of short M–O bonds in the  $\text{MO}_6$  octahedron that protrude into the structure spaces. The peak at  $538\text{ cm}^{-1}$  is assorted with internal vibrations of the oxygen tetrahedron. Raman scattering of  $\text{ZnSnO}_3$ /PMMA composite film (shown in Fig. 7) exhibits only one Raman active mode at  $279\text{ cm}^{-1}$  from  $\text{ZnSnO}_3$  while other Raman modes noticed in the spectra are from PMMA [37, 38].

The FTIR spectra of both  $\text{ZnSn(OH)}_6$  and  $\text{ZnSnO}_3$  are shown in Fig. 8. The bands at  $\sim 3213\text{ cm}^{-1}$  is ascribed to the bending and stretching vibration modes of hydroxyl (–OH) group in the structure of  $\text{ZnSn(OH)}_6$ . The bands at  $779$ ,  $848$ ,  $1176$ , and  $\sim 2309\text{ cm}^{-1}$  may be attributed to



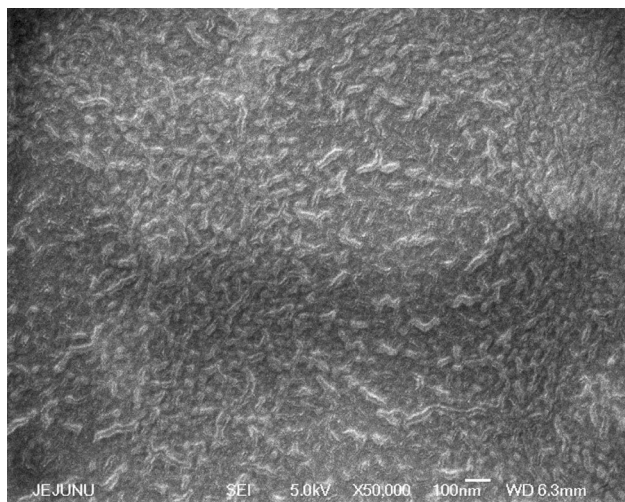


**Fig. 5** FE-SEM image of ZnSnO<sub>3</sub>/PMMA composite film deposited on PET by electro spray deposition method

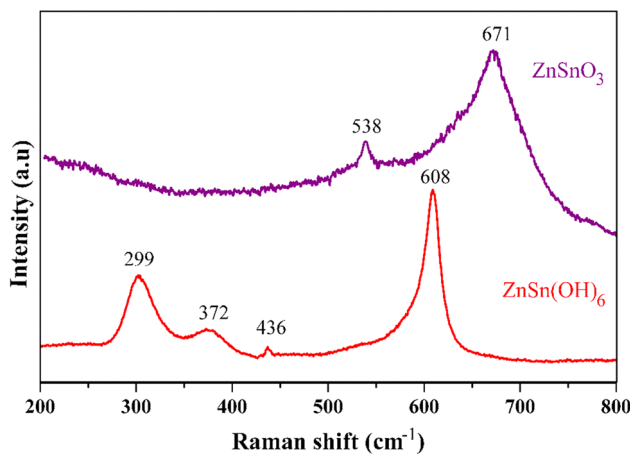


**Fig. 6** Raman spectra of ZnSn(OH)<sub>6</sub> and ZnSnO<sub>3</sub> nanocubes showing shifting of four Raman modes to two new Raman modes after calcination at 600 °C for 3 h

vibration of M–O or M–OH–M groups for ZnSn(OH)<sub>6</sub> while the bands at 533, 572, and 1113 cm<sup>-1</sup> are assigned to vibrations of M–O or M–O–M groups for ZnSnO<sub>3</sub>. It was observed from the spectral data that, after calcination the peaks of the (–OH) group almost disappeared while the peaks attributed to the M–O bond became prominent which testified the conversion of ZnSn(OH)<sub>6</sub> into ZnSnO<sub>3</sub>. The FTIR spectra of ZnSnO<sub>3</sub>–PMMA composite film is shown in Fig. 9, in which both ZnSnO<sub>3</sub> and PMMA peaks are present, but most of the peaks belong to PMMA and agree well with the values of the FTIR spectra of PMMA reported in the literature [17, 39]. The peaks at 538 and 617 cm<sup>-1</sup> are attributed to the vibrations of M–O or M–O–M groups for ZnSnO<sub>3</sub>. The peaks at 696 and 750 cm<sup>-1</sup> are assigned to out of plane OH bending. The band at

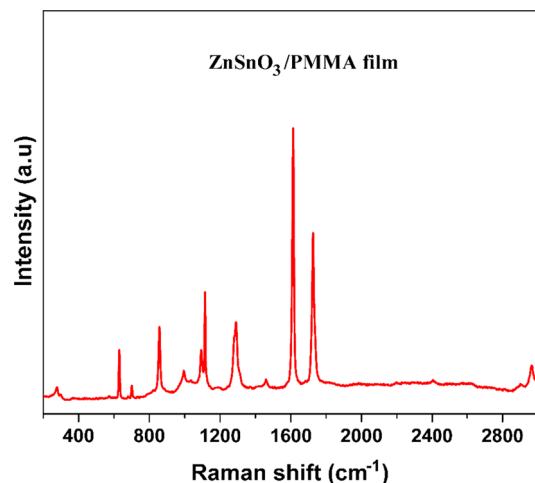


**Fig. 7** Raman spectra of ZnSnO<sub>3</sub>/PMMA composite film showing only one Raman active mode at 279 cm<sup>-1</sup> from ZnSnO<sub>3</sub> while others belong to PMMA

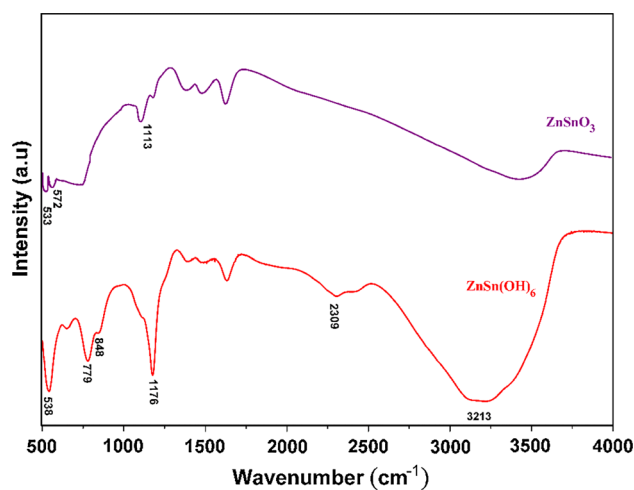


**Fig. 8** FTIR spectra of ZnSn(OH)<sub>6</sub> and ZnSnO<sub>3</sub> nanocubes exhibiting the conversion of ZnSn(OH)<sub>6</sub> to ZnSnO<sub>3</sub>

987 cm<sup>-1</sup> is the characteristic absorption of PMMA, together with the band at 1067 cm<sup>-1</sup>. The peak observed at 1151 cm<sup>-1</sup> is assigned to C–O stretching, whereas the peak observed at 1452 cm<sup>-1</sup> is assigned to O–CH<sub>3</sub> bending and at 1733 cm<sup>-1</sup> is attributed to C=O stretching which shows the presence of the acrylate carboxyl group. The two peaks at 2850 and 2924 cm<sup>-1</sup> are assigned to C–H stretching vibrations. The other two peaks at 3446 and 1541 cm<sup>-1</sup> can be attributed to the –OH group stretching and bending vibrations of physisorbed moisture [40].

### 3.3 Optical characterization

Transmittance and absorbance of as deposited ZnSnO<sub>3</sub>/PMMA composite film on PET was carried out by using

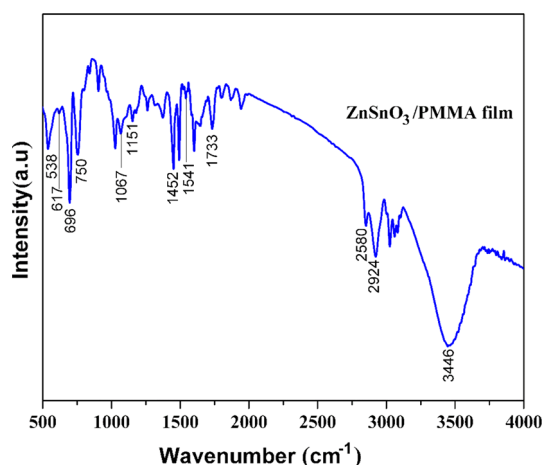


**Fig. 9** FTIR spectra of ZnSnO<sub>3</sub>/PMMA composite film on PET showing two peaks 538 and 617 cm<sup>-1</sup> from ZnSnO<sub>3</sub> and others are from PMMA

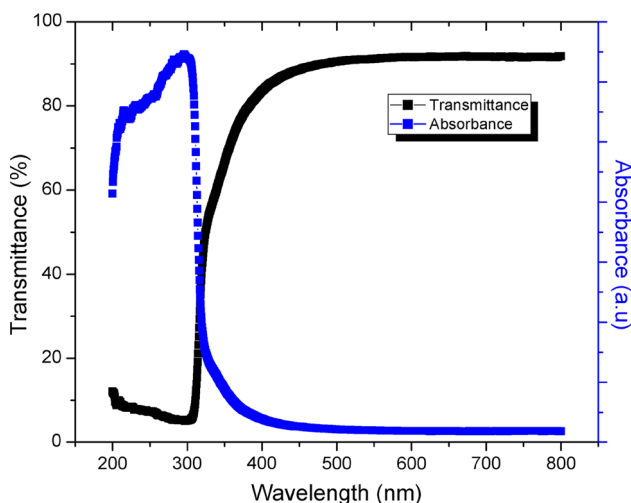


**Fig. 10** Transmittance and absorbance spectrums of ZnSnO<sub>3</sub>/PMMA deposited film on PET by ESD

UV–Vis–NIR spectrophotometer as shown in Fig. 10. It shows the high transmittance and low absorbance of the deposited film of ZnSnO<sub>3</sub>/PMMA on PET. It shows an average transmittance of 92 %, which indicates that it can be very useful in transparent electronics.

### 3.4 Electrical characterization

Electrical properties of ZnSnO<sub>3</sub>/PMMA composite film were measured by semiconductor device analyzer by placing the probes of device on silver contacts deposited on the ZnSnO<sub>3</sub>/PMMA composite film so that they may not damage the film. The *I*–*V* plot for an approximately 149 nm thick ZnSnO<sub>3</sub>/PMMA composite film is shown in Fig. 11. The *I*–*V* plot shows very low currents and high

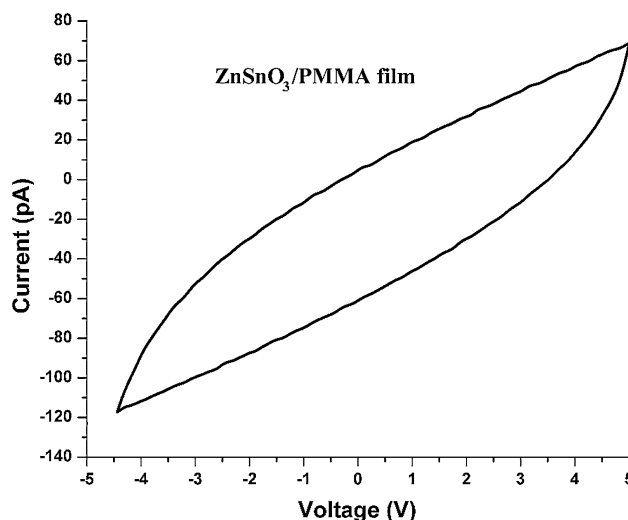


**Fig. 11** *I*–*V* characteristic curve exhibiting the dielectric behavior of ZnSnO<sub>3</sub>/PMMA composite film on PET with non-linear behavior and low magnitude of current

resistance at applied potentials from –5 to 5 V. The resistivity was measured from the slopes of the *I*–*V* plot and using the sheet resistivity formula for thin films:

$$\rho = \frac{\pi t}{\ln 2} \left( \frac{V}{I} \right) \tag{4}$$

where ‘*t*’ is the thickness of the film (149 nm), while ‘*V*’ is voltage and ‘*I*’ is the current from the *I*–*V* plot. The calculated resistivity was found out to be  $\approx 50 \times 10^5 \Omega \text{ cm}$ . As a passive component this material can be used as dielectric layer for a wide range of electronic devices.

## 4 Conclusion

In this work, we first synthesized the ZnSnO<sub>3</sub> nanocubes with an average size of 50–70 nm via an aqueous solution method on suitable conditions. The surface morphology, crystal structure and composition of intermediate product ZnSn(OH)<sub>6</sub> and final product ZnSnO<sub>3</sub> nanocubes were investigated by carrying out the FE-SEM, XRD, Raman and FTIR characterizations and difference between the two phases was illustrated with the help of obtained data. And then ZnSnO<sub>3</sub> nanocubes were dispersed in the PMMA solution to make the ZnSnO<sub>3</sub>/PMMA ink. This ink was then sprayed on a flexible substrate PET by electro spray deposition (ESD) method. The thickness of the film was measured and found to be approximately 149 nm. The FE-SEM, XRD, UV/Vis/NIR, FTIR, Raman spectroscopy and *I*–*V* tests were conducted of the as deposited ZnSnO<sub>3</sub>/PMMA composite film. The transmittance of the film was approximately 92 % and calculated resistivity of the thin film with thickness of 149 nm was  $50 \times 10^5 \Omega \text{ cm}$ .

**Acknowledgments** This work was supported by the Nano-Convergence Foundation (commercialization of the hard coating/index matching film for touch panel ITO film) funded by the Ministry of Science, ICT and Future Planning (MSIP, Korea) and the Ministry of Trade, Industry and Energy (MOTIE, Korea).

## References

1. K.Y. Lee, D. Kim, J.-H. Lee, T.Y. Kim, M.K. Gupta, S.-W. Kim, *Adv. Funct. Mater.* **24**, 37 (2014)
2. J.M. Wu, C. Xu, Y. Zhang, Z.L. Wang, *ACS Nano* **6**, 4335 (2012)
3. J.M. Wu, C. Xu, Y. Zhang, Y. Yang, Y. Zhou, Z.L. Wang, *Adv. Mater.* **24**, 6094 (2012)
4. H. Fan, Y. Zeng, X. Xu, N. Lv, T. Zhang, *Sens. Actuators B Chem.* **153**, 170 (2011)
5. Y. Chen, L. Yu, Q. Li, Y. Wu, Q. Li, T. Wang, *Nanotechnology* **23**, 415501 (2012)
6. P. Song, Q. Wang, Z. Yang, *Sens. Actuators B Chem.* **156**, 983 (2011)
7. J.M. Wu, C.-Y. Chen, Y. Zhang, K.-H. Chen, Y. Yang, Y. Hu, J.-H. He, Z.L. Wang, *ACS Nano* **6**, 4369 (2012)
8. S.-J. Seo, C.G. Choi, Y.H. Hwang, B.-S. Bae, *J. Phys. D Appl. Phys.* **42**, 035106 (2009)
9. H.Q. Chiang, J.F. Wager, R.L. Hoffman, J. Jeong, D.A. Keszler, *Appl. Phys. Lett.* **86**, 013503 (2005)
10. B. Tan, E. Toman, Y. Li, Y. Wu, *J. Am. Chem. Soc.* **129**, 4162 (2007)
11. Y.-Y. Choi, K.-H. Choi, H. Lee, H. Lee, J.-W. Kang, H.-K. Kim, *Sol. Energy Mater. Sol. Cells* **95**, 1615 (2011)
12. D. Kovacheva, K. Petrov, *Solid State Ionics* **109**, 327 (1998)
13. D.L. Young, H. Moutinho, Y. Yan, T.J. Coutts, *J. Appl. Phys.* **92**, 310 (2002)
14. S. Yu-sheng, Z. Tian-shu, *Sens. Actuators B* **12**, 5 (1993)
15. X.Y. Xue, Y.J. Chen, Q.H. Li, C. Wang, Y.G. Wang, T.H. Wang, *Appl. Phys. Lett.* **88**, 182102 (2006)
16. B. Liu, H.C. Zeng, *Langmuir* **20**, 4196 (2004)
17. B. Chandar Shekar, S. Sathish, B.T. Bhavyasree, B. Ranjith Kumar, *Adv. Mater. Res.* **678**, 309 (2013)
18. S. Uemura, M. Yoshida, S. Hoshino, T. Kodzasa, T. Kamata, *Thin Solid Films* **438–439**, 378–381 (2003)
19. D. Alobaidani, D. Furniss, M.S. Johnson, A. Endruweit, A.B. Seddon, *Opt. Lasers Eng.* **48**, 575 (2010)
20. A. Okada, A. Usuki, *Mater. Sci. Eng. C* **3**, 109 (1995)
21. J.W. Gilman, *Appl. Clay Sci.* **15**, 31 (1999)
22. S. Kim, J. Ok, M. Ahn, D. Park, G. Lee, *Trans. Electr. Electron. Mater.* **3**, 9 (2002)
23. A.A. Novakova, V.Y. Lanchinskaya, A.V. Volkov, T.S. Gendler, T.Y. Kiseleva, M.A. Moskvina, S.B. Zezin, *J. Magn. Magn. Mater.* **258–259**, 354–357 (2003)
24. M. Mustafa, H.C. Kim, H.D. Yang, K.H. Choi, *J. Mater. Sci. Mater. Electron.* **24**, 4321 (2013)
25. N.M. Muhammad, S. Sundharam, H.-W. Dang, A. Lee, B.-H. Ryu, K.-H. Choi, *Curr. Appl. Phys.* **11**, S68 (2011)
26. M. Mustafa, M.N. Awais, G. Pooniah, K.H. Choi, J. Ko, Y.H. Doh, *J. Korean Phys. Soc.* **61**, 470 (2012)
27. N.M. Muhammad, A.M. Naeem, N. Duraisamy, D.-S. Kim, K.-H. Choi, *Thin Solid Films* **520**, 1751 (2012)
28. K.-H. Choi, M. Mustafa, J.-B. Ko, Y.-H. Doh, *Thin Solid Films* **525**, 40 (2012)
29. K.H. Choi, N.M. Muhammad, H.W. Dang, A. Lee, J.S. Hwang, J.W. Nam, B.H. Ryu, *Int. J. Mater. Res.* **102**, 1252 (2011)
30. S. Khan, Y.H. Doh, A. Khan, A. Rahman, K.H. Choi, D.S. Kim, *Curr. Appl. Phys.* **11**, S271 (2011)
31. M. Maria, D. Navaneethan, K.H. Chan, H.M. Taek, C.K. Hyun, *Appl. Phys. A* **109**, 515 (2012)
32. A. Ali, K. Ali, K.-R. Kwon, M.T. Hyun, K.H. Choi, *J. Mater. Sci. Mater. Electron.* **25**, 1097 (2013)
33. M. Mustafa, H.C. Kim, Y.H. Doh, K.H. Choi, *Polym. Eng. Sci.* **54**, 675–681 (2014)
34. K.-H. Choi, K. Rahman, N.M. Muhammad, A. Khan, K.-R. Kwon, Y.-H. Doh, H.-C. Kim, in *Recent Advances in Nanofabrication Techniques and Applications*, ed. by B. Cui (2011). doi:10.5772/24672
35. H. Fan, S. Ai, P. Ju, *Cryst. Eng. Comm.* **13**, 113 (2011)
36. J. Zeng, M. Xin, H. Wang, H. Yan, W. Zhang, *J. Phys. Chem. C* **112**, 4159 (2008)
37. K.J. Thomas, M. Sheeba, V.P.N. Nampoore, C.P.G. Vallabhan, P. Radhakrishnan, *J. Opt. A Pure Appl. Opt.* **10**, 055303 (2008)
38. C. Hu, S. Chen, W. Zhang, F. Xie, J. Chen, X. Chen, *J. Raman Spectrosc.* **44**, 1136 (2013)
39. S. Sathish, B. Shekar, *Indian J. Pure Appl. Phys.* **52**, 64 (2014)
40. G. Duan, C. Zhang, A. Li, X. Yang, L. Lu, X. Wang, *Nanoscale Res. Lett.* **3**, 118 (2008)